

Supplementary Information: Charge-transfer and
impulsive electronic-to-vibrational energy
conversion in ferricyanide: ultrafast photoelectron
and transient infrared studies

José Ojeda,^a Christopher A. Arrell,^a Luca Longetti,^a Majed Chergui,^a
and Jan Helbing^b

Contents

1 UV-VIS and IR absorption spectra of solvated ferricyanide	S2
2 Decay-associated spectra	S3
3 Pump intensity-dependence (266 nm excitation)	S4

1 UV-VIS and IR absorption spectra of solvated ferricyanide

As there is a vacancy in the t_{2g} level, the ground state of the complex has ${}^2T_{2g}$ symmetry. UV-VIS absorption spectra of ferricyanide in the solvents considered in this study are shown in Fig. S1. In H_2O and D_2O , the LMCT bands are located at ~ 260 , 302 and 420 nm and are assigned to ${}^2T_{2g} \rightarrow {}^2T_{1u}(t_{1u} \rightarrow t_{2g})$, ${}^2T_{2g} \rightarrow {}^2T_{2u}(t_{2u} \rightarrow t_{2g})$ and ${}^2T_{2g} \rightarrow {}^2T_{1u}(t_{1u} \rightarrow t_{2g})$, respectively [S1, S2, S3, S4]. These bands are slightly red shifted for ethylene glycol solutions.

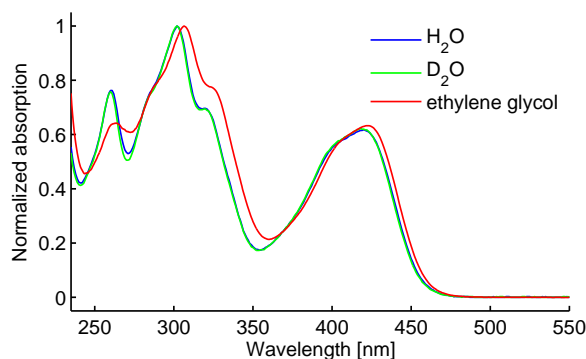


Figure S1: Normalized UV-VIS absorption spectrum of ferricyanide in the solvents used in this study.

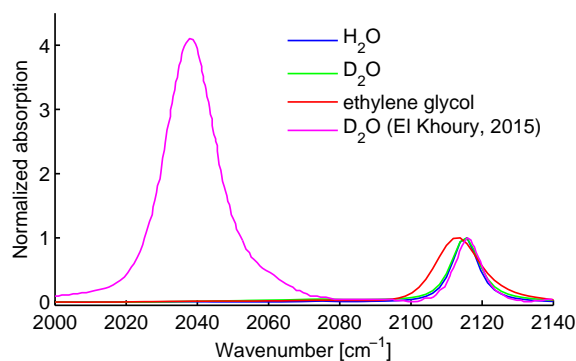


Figure S2: IR absorption spectrum of ferricyanide in the solvents used in this study, normalized at the CN stretch band. The scaled magenta spectrum (adapted from reference [S5]) contains contributions from identical concentrations of ferro- and ferricyanide in D_2O .

Fig. S2 shows IR spectra of ferricyanide in the different solvents considered in this study, after normalization at the (T_{1u}) CN stretch band. A scaled spectrum of a D_2O sample containing identical concentrations of ferricyanide and ferrocyanide (see reference [S5]) is shown for illustrating the much stronger oscillator strength associated to the Fe^{2+} species (at ~ 2036 cm^{-1}).

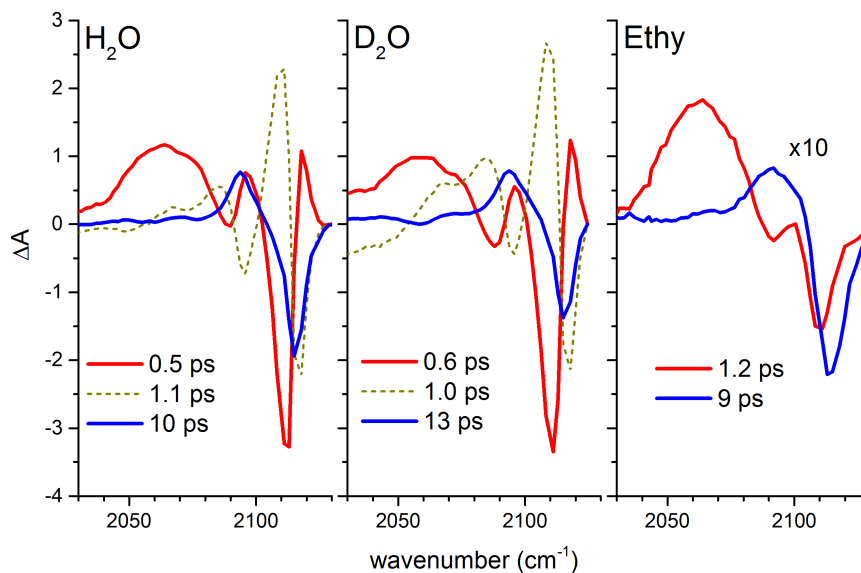


Figure S3: Decay-associated spectra for the global fit of the data shown in Fig. 3 of the main paper and belonging to the time-constants shown in table 1.

2 Decay-associated spectra

Fig S3 shows the decay-associated spectra (DAS) for the global fit of the data shown in Fig. 3 of the main paper. The DAS for the shortest time constant (red) reflect the decay of the broad excited state absorption at 2065 cm^{-1} alongside fast recovery of the $v = 0$ bleach at 2115 cm^{-1} . The 1 ps second spectra in water (dashed lines) exhibit an oscillatory pattern typical of spectral shifts. In the bleach region it is balancing much of the first DAS, indicating that no simple exponential kinetics describes the spectral evolution at these wavenumbers, and that only the 2065 cm^{-1} decay can be uniquely associated with the the fastest time constant. The long time signals (blue) nicely shows the decay of the $v = 1 \rightarrow v = 2$ band (with a small contribution from $v = 2 \rightarrow v = 3$ in water) and the recovery of the vibrational ground state. While the global exponential fit provides a good idea about the timescales involved, the time-constants for vibrational decay are more reliably obtained from the model fits shown in Fig. 4 of the paper.

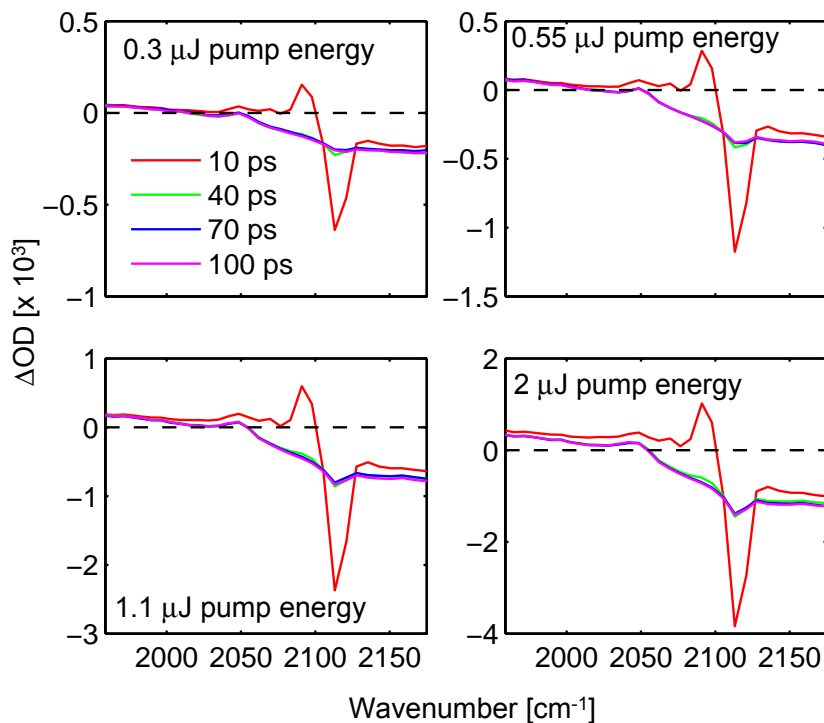


Figure S4: TA-IR spectra at different intensities of the 266 nm pump pulse.

3 Pump intensity-dependence (266 nm excitation)

Raw TA-IR spectra (H₂O, 266 nm excitation) at four different pump-probe delays are shown in Fig. S4. Each graph corresponds to a different intensity of the 266 nm pump pulse in order to check the linearity of the signal. The tilt of the baseline is due to the temperature rise in the solvent. We take the difference between the peaks near 2090 cm⁻¹ and 2115 cm⁻¹ as a measure for the ferricyanide response (red squares Fig. S5, 'IR') and the difference between the baseline at 2170 cm⁻¹ and 1960 cm⁻¹ as a measure for the solvent response (cyan triangles in Fig. S5, 'heat'). Both increase linearly with pump-intensity and their ratio (gray bars) is constant.

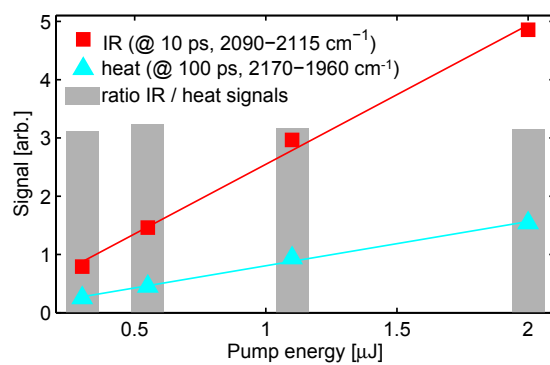


Figure S5: Linearity check: ferricyanide signal (red square) and heat signal (cyan triangles) as a function of 266 nm pump energy in H₂O. Data extracted from Fig. S4 as explained in the text.

References

- [S1] Alexander, J. J.; Gray, H. B. *J. Am. Chem. Soc.* **1968**, *90*, 4260–4271.
- [S2] Gale, R.; McCaffery, A. J. *J. Chem. Soc., Dalton Trans.* **1973**, 1344–1351.
- [S3] Upton, A. H.; Williamson, B. E. *J. Phys. Chem.* **1994**, *98*, 71–76.
- [S4] Bolvin, H. *J. Phys. Chem. A* **1998**, *102*, 7525–7534.
- [S5] El Khoury, Y.; Van Wilderen, L. J.; Vogt, T.; Winter, E.; Bredenbeck, J. *Rev. Sci. Inst.* **2015**, *86*, 083102.